Adsorption (2011) 17:889–900
DOI 10.1007/s10450-011-9357-z

A model for enhanced coal bed methane recovery aimed at carbon dioxide storage

The role of sorption, swelling and composition of injected gas

Ronny Pini · Giuseppe Storti · Marco Mazzotti

Received: 9 October 2010 / Accepted: 8 March 2011 / Published online: 24 March 2011

Abstract Numerical simulations on the performance of CO_2 storage and enhanced coal bed methane (ECBM) recovery in coal beds are presented. For the calculations, a one-dimensional mathematical model is used consisting of mass balances describing gas flow and sorption, and a geomechanical relationship to account for porosity and permeability changes during injection. Important insights are obtained regarding the gas flow dynamics during displacement and the effects of sorption and swelling on the ECBM operation. In particular, initial faster CH_4 recovery is obtained when N_2 is added to the injected mixture, whereas pure CO_2 allows for a more effective displacement in terms of total CH_4 recovery. Moreover, it is shown that coal swelling dramatically affects the gas injectivity, as the closing of the fractures associated with it strongly reduces coal's permeability. As a matter of fact, injection of flue gas might represent a useful option to limit this problem.

Keywords ECBM · Simulation · Permeability · Sorption · Swelling

R. Pini (✉) · M. Mazzotti
Institute of Process Engineering, ETH Zurich, Sonneggstrasse 3, 8092 Zurich, Switzerland
e-mail: marco.mazzotti@ipe.mavt.ethz.ch

Present address:
R. Pini
Department of Energy Resources Engineering, Stanford University, 367 Panama Street, Stanford, CA 94305, USA
e-mail: pini@stanford.edu

G. Storti
Dipartimento di Chimica, Materiali e Ing. Chimica "Giulio Natta", Sede Mancinelli, Politecnico di Milano, Via Mancinelli 7, 20131 Milano, Italy

Notation

A	Cross sectional area [m^2]
b	Langmuir equilibrium constant [1/Pa]
b^s	Langmuir equilibrium constant (swelling)) [1/Pa]
c	Gas phase concentration [mol/m^3]
C_1	Effective pressure coefficient [1/Pa]
C_2	Swelling coefficients [–]
F	Molar flow rate [mol/day]
GIP	Original Gas In Place [mol]
i	Component i
I	Amount injected [mol]
k	Permeability [m^2], 1 mD $= 9.869233 \times 10^{-16}$ m^2
k_m	Mass transfer coefficient [1/s]
k_{ij}	Interaction parameter (Peng Robinson) [–]
L	Coal bed length [m]
n	Adsorbed phase concentration [mol/m^3]
n^*	Equilibrium adsorbed phase concentration [mol/m^3]
n^∞	Saturation capacity per unit mass adsorbent [mol/g]
n_c	Number of components [–]
P	Gas phase pressure [Pa]
P_c	Confining pressure [Pa]
Pu	Purity [%]
R	Recovery factor [%]
s	Volumetric swelling [–]
s^∞	Saturation capacity (swelling) [–]
S	Amount stored [mol]
t	Time [s]
T	Temperature [°C]
u	Superficial fluid velocity [m/s]
v	Interstitial fluid velocity [m/s]
w	Acentric factor (Peng Robinson) [–]
y	Gas phase molar fraction [m^3/mol]
z	Axial coordinate [m]

Greek Letters

α Swelling isotherm coefficient [m^3/mol]
β Swelling isotherm coefficient [–]
ε Fractures (cleats) porosity [–]
ε^* Total porosity [–]
ε_p Macropores porosity [–]
μ Dynamic viscosity [Pa.s]
ρ_s Coal bulk density [kg/m^3]

1 Introduction

Over the next 20 years from now, natural gas will play a key role in the power sector, mainly because of its availability and its low carbon content with respect to oil and coal (IEA 2009). At the same time, there is the need to develop technologies where the produced carbon dioxide (CO_2) is captured and subsequently stored (Carbon dioxide Capture and Storage, CCS), thus allowing the continued use of fossil fuels, while reducing their impact on the increase of atmospheric CO_2 concentration (IPCC 2005). The increasing need of natural gas has stimulated the exploration of the so-called unconventional gas resources, namely tight sands, gas shales and coal bed methane (CBM) (IEA 2009). Among these, the latter is very attractive as the coal seams that have retained the methane (CH_4) for million of years might be exploited as geological storage repositories for CO_2. In fact, it is well known from coal mining that significant amounts of gas can be retained in these reservoirs both by adsorption on the coal surface as well as by absorption into the coal's solid matrix (Rice 1993). Moreover, injection of CO_2 into the coal seam would enhance the recovery of CH_4, as the former has a stronger affinity to coal compared to the latter (White et al. 2005). This process is called Enhanced Coal Bed Methane recovery, and, as for enhanced oil recovery, it allows in principle offsetting the costs associated to the CCS operation (Mazzotti et al. 2009). Moreover, the injection of flue gas into a coal bed for ECBM recovery might be an attractive alternative to pure CO_2 injection for several reasons. First, flue gas is the combustion exhaust gas produced by power plants, and it could therefore be directly injected, thus avoiding the expensive capture step. Secondly, flue gas consists of mostly nitrogen (87%) and carbon dioxide (13%); the presence of the weakly adsorbing N_2 would allow keeping the coal permeability sufficiently high (Bustin et al. 2008; Durucan and Shi 2009). This option's obvious drawback would be the need to compress not only CO_2 but also nitrogen before injection.

Observations from the performed field tests evidence that the interactions between the gas and the coal need to be better understood if ECBM technology has to be deployed at a commercial scale (Gunter et al. 2004; Reeves 2004; Shi et al. 2008; van Bergen et al. 2009). Among these, gas sorption and swelling have complex effects on the displacement dynamics, whose accurate description is essential for the development of reliable reservoir simulators used to history match field test data obtained from ECBM field tests. Input for these models are the results of laboratory studies that have focused on the different aspects related to CO_2 storage in coal seams, namely gas sorption (Bae and Bhatia 2006; Day et al. 2008a; Pini et al. 2010), coal swelling (St. George and Barakat 2001; Day et al. 2008b; Ottiger et al. 2008) and permeability changes upon gas injection (Wang et al. 2007; Mazumder and Wolf 2008; Pini et al. 2009).

One dimensional models have been shown to provide a very useful understanding of the key mechanisms that affect the storage and recovery process (Gilman and Beckie 2000; Shi and Durucan 2003; Wang et al. 2007; Jessen et al. 2008; Seto et al. 2009). One can distinguish up to four types of pores in coal, namely cleats where gas and water are present, macro- and mesopores where there is only free gas, and micropores where adsorption takes place. The general assumption is that the displacement of CH_4 by CO_2 results from a multistep process. The gas injected in the coal bed diffuses from the fracture network through the matrix and macropores and finally to the internal surface of the coal. Here, partial pressure with respect to the adsorbed gas is reduced, causing desorption, and gas exchange takes place. Finally, the desorbed gas diffuses back through the matrix and micropores, out to the fracture network where it flows to the production well (Gentzis 2000; Totsis et al. 2004). This mass transfer can be described through a linear driving force model by lumping gas diffusion in the different types of pore using a single mass transfer coefficient, or the corresponding time constant (Bromhal et al. 2005; Sams et al. 2005).

In a previous work, a model was derived that includes this relatively simple description of mass transfer complemented by the description of porosity and permeability changes in the coal during injection. This model was successfully applied for describing pure gas injection experiments into coal cores confined under an external hydrostatic pressure and under simulated reservoir temperature and pressure conditions (Pini et al. 2009).

In the present study, this model is extended to the multicomponent single-phase (gas) displacement in a coal seam and numerical simulations estimating the performance of CO_2 storage and ECBM recovery in coal beds are presented. In particular, different ECBM scenarios involving the injection of gas mixtures with different composition (from pure N_2 to pure CO_2) into a coal bed previously saturated with methane are investigated. Moreover, emphasis will be placed on the effects of the sorption-induced swelling on the coal bed permeability and on its consequences on the CO_2 storage operation itself.

2 Modeling

The following assumptions are introduced in the development of the model: (a) the system is isothermal; (b) all the mechanical and physicochemical properties are constant and homogeneously distributed; (c) the coal behaves as an isotropic linear poroelastic medium; (d) single-phase (gas) flow is considered. The latter assumption is justified by considering the situation where gas injection starts at the end of the so-called primary recovery operation. In fact, during primary recovery almost all the water originally present in the reservoir is removed and the remaining fraction can be safely considered immobile (Zhu et al. 2003; Durucan and Shi 2009). In the following the two main components that constitute the model are presented, namely the mass balances accounting for gas flow and sorption, and the stress-strain relationship for the description of porosity and permeability changes during injection.

2.1 Mass balances

Coal reservoirs are fractured systems consisting of a low permeability matrix and a high permeability fracture (cleat) network. In this study, the coal total porosity ε^* is divided into cleat porosity ε and macroporosity ε_p, with the microporosity being accounted for as combined with the solid material, i.e.

$$\varepsilon^* = \varepsilon + (1-\varepsilon)\varepsilon_p \tag{1}$$

Since the sorption process is assumed to be the rate limiting step, the gas concentration and pressure in the macropores and in the fractures are set to be the same. For a system of n_c components, material balances are written for each component i:

$$\frac{\partial(\varepsilon^* c_i)}{\partial t} + \frac{\partial[(1-\varepsilon^*)n_i]}{\partial t} + \frac{\partial(uc_i)}{\partial z} = 0, \quad i = 1,\ldots,n_c \tag{2}$$

where c_i and n_i are respectively the actual gas and adsorbed phase concentration of component i, u is the superficial velocity, and t and z are time and space coordinates. Note that in (2) axial dispersion is neglected, as in this study the situation is considered of continuous injection, where a pressure gradient of about 4 MPa across the coal seam exists for the whole duration of the operation. Under such conditions, diffusive effects in the fractures are negligible and the flow is dominated by convection. An conservative analysis of the Peclet number, i.e. the ratio of the characteristic time for convection to the characteristic time for diffusion, supports this conclusion; for the conditions applied in this study and a diffusion coefficient of 10^{-5} m^2/s, the resulting Peclet number takes a value of at least 600, i.e. much larger than one, a situation under which axial mixing can be safely neglected.

A linear driving force model is used to describe the sorption rate of component i through the coal's matrix, i.e.

$$\frac{\partial[(1-\varepsilon^*)n_i]}{\partial t} = (1-\varepsilon^*)k_{mi}(n_i^* - n_i), \quad i = 1,\ldots,n_c \tag{3}$$

where k_{mi} is the mass transfer coefficient of component i. The driving force for gas sorption is given by the difference between the equilibrium adsorbed phase concentration of component i, n_i^*, and the actual concentration of component i in the adsorbed phase, n_i, the former being described by an equilibrium adsorption isotherm, i.e.

$$n_i^* = \rho_s \frac{n_i^\infty b_i y_i P}{1 + P\sum_{j=1}^{n_c} b_j y_j}, \quad i = 1,\ldots,n_c \tag{4}$$

where n_i^* is the adsorbed concentration of component i in the solid material per unit volume coal, ρ_s is the adsorbent bulk density, y_i is the gas molar fraction and P is the pressure; n_i^∞ and b_i are the saturation capacity per unit mass adsorbent and the Langmuir equilibrium constant of component i, respectively.

The superficial velocity u is given by Darcy's law:

$$u = v\varepsilon = -\frac{k}{\mu}\left(\frac{\partial P}{\partial z}\right) \tag{5}$$

where v is the interstitial velocity, k the permeability and μ the dynamic viscosity.

2.2 Stress-strain relationship

A stress-strain constitutive equation is required to describe the mechanical behavior of the coal bed during the injection operation. The fluid pressure in the coal bed plays a decisive role in determining the stress situation of the reservoir, thus affecting markedly the porosity and the permeability of the porous medium (Gray 1987; Cui et al. 2007).

First, fractures are closed or widened, depending on whether the effective pressure on the rock (defined as the lithostatic overburden minus the fluid pressure) is increased or reduced. Secondly, upon gas sorption the coal swells thus reducing the fracture openings. In the case of coal such an equation has been shown to take the following general form (Gilman and Beckie 2000; Shi and Durucan 2004; Bustin et al. 2008):

$$\frac{k}{k_0} = \left(\frac{\varepsilon}{\varepsilon_0}\right)^3 = \exp\left[-C_1(P_c - P) - C_2 s\right] \tag{6}$$

where P is the gas pressure, P_c is the confining pressure (lithostatic overburden), s is total swelling, and C_1 and C_2 are coefficients that depend on coal properties. The subscript 0 refers to an arbitrarily chosen initial state. In this study, the reference values of porosity and permeability apply to

an unstressed coal in contact with a non-swelling gas at atmospheric pressure. It is worth pointing out, that the experimental validation of (6) has been recently reported for high pressure gas injection experiments on coal cores confined by an external pressure (Pini et al. 2009).

Several studies have shown that coal swelling can be effectively described by a Langmuir-like equation (Levine 1996; Palmer and Mansoori 1998; Shi and Durucan 2004; Cui et al. 2007; Pini et al. 2009). In an analogous way as for sorption of gas mixtures, an extended Langmuir equation is applied to coal's swelling:

$$s_i = \frac{s_i^{\infty} b_i^{\mathrm{s}} y_i P}{1 + P \sum_{j=1}^{n_c} b_j^{\mathrm{s}} y_j}, \quad i = 1, \ldots, n_c \tag{7}$$

with s_i^{∞} and b_i^{s} being the corresponding isotherm parameters. To preserve the physical connection between sorption and swelling, (7) and (4) are combined to obtain an equation expressing the total swelling as a function of gas sorption, allowing therefore to account for the kinetic of the swelling process through the sorption rate given by (3):

$$s = \sum_{i=1}^{n_c} s_i = \frac{\sum_{i=1}^{n_c} \alpha_i \beta_i n_i}{1 - \sum_{j=1}^{n_c} \alpha_i n_i} \tag{8}$$

where the parameters α_i and β_i are functions of the Langmuir parameters of the sorption and swelling isotherms, i.e.

$$\alpha_i = \frac{b_i - b_i^{\mathrm{s}}}{\rho_{\mathrm{s}} n_i^{\infty} b_i}, \quad i = 1, \ldots, n_c \tag{9a}$$

$$\beta_i = \frac{b_i^{\mathrm{s}} s_i^{\infty}}{b_i - b_i^{\mathrm{s}}}, \quad i = 1, \ldots, n_c \tag{9b}$$

Note that (8) is valid for $0 \le n_i \le n_i^{\infty}$.

3 Solution procedure

The problem is defined by (1)–(6) and it is completed by the following constitutive equations: (a) the Peng-Robinson EOS, needed to relate gas density to pressure and temperature (Peng and Robinson 1976) and (b) a relationship for the gas mixture viscosity following the method of Wilke (Reid et al. 1987). Initial and boundary conditions are defined as follows:

Initial conditions: at $t = 0$, $c_i = c_i^0$, $0 \le z \le L$

$$n_i = n_i^0, \ 0 \le z \le L$$

Boundary conditions: at $z = 0$, $c_i = c_i^{\mathrm{inj}}$, $t > 0$

at $z = L$, $P = P_{\mathrm{out}}$, $t > 0$

The orthogonal collocation method has been applied to discretize in space the partial differential equations (Villadsen and Michelsen 1978; Morbidelli et al. 1983). The resulting system of ordinary differential equations has then been solved numerically using a commercial ODEs solver (in Fortran).

3.1 Parameters estimation

An extensive set of experimental data for the sorption, swelling and permeability behavior of an Italian coal from the Sulcis Coal Province (Sardinia, Italy) has been produced and published (Ottiger et al. 2006; Ottiger et al. 2008; Pini et al. 2009). With reference to the present work, the measured sorption and swelling isotherms of CO_2, CH_4 and N_2 have been fitted by the Langmuir model and they are shown in Fig. 1. Note that prior fitting the measured excess sorption isotherms have been converted to absolute sorption

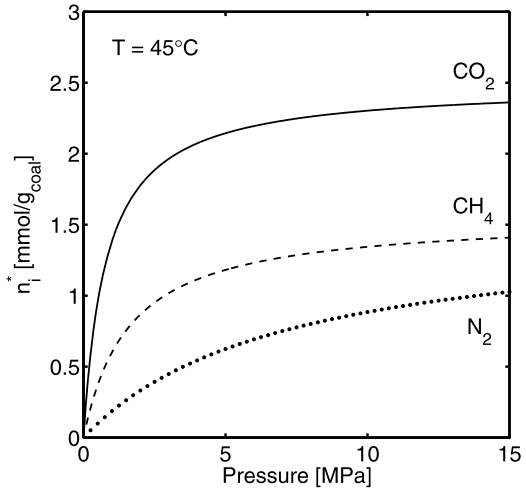

(a) Sorption isotherms

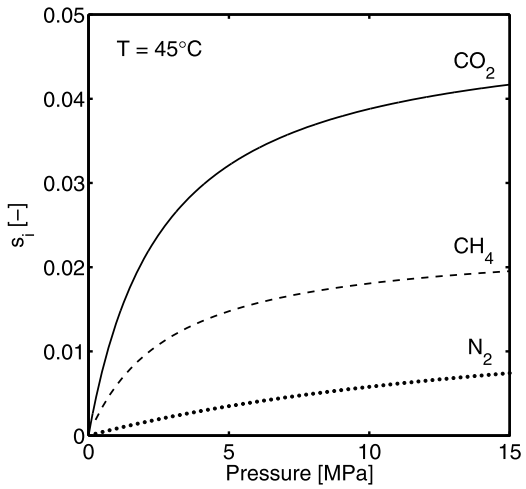

(b) Swelling isotherms

Fig. 1 Langmuir sorption (**a**) and swelling (**b**) isotherms at 45°C as a function of pressure for CO_2 (*solid line*), CH_4 (*dashed line*) and N_2 (*dotted line*) for a coal from the Sulcis coal province

Table 1 Langmuir constants for the sorption and swelling isotherms for the coal considered in this study

	Sorption isotherm		Swelling isotherm	
	n_i^∞ [mol/g]	b_i [Pa^{-1}]	s_i^∞ [–]	b_i^s [Pa^{-1}]
CO_2	2.49×10^{-3}	1.25×10^{-6}	4.90×10^{-2}	3.80×10^{-7}
CH_4	1.56×10^{-3}	6.26×10^{-7}	2.33×10^{-2}	3.47×10^{-7}
N_2	1.52×10^{-3}	1.40×10^{-7}	1.70×10^{-2}	5.19×10^{-8}

Table 2 Constants C_1 (Pa^{-1}) and C_2 of (6) as obtained from different permeability models

Reference	C_1	C_2
Gilman and Beckie (2000)	$\frac{3\nu}{E_f(1-\nu)}$	$\frac{3E_Y}{(1-\nu)E_f}$
Shi and Durucan (2004)	$\frac{3C_f\nu}{(1-\nu)}$	$\frac{C_fE_Y}{(1-\nu)}$
Bustin et al. (2008)	$\frac{1+\nu}{K\varepsilon_0(1-\nu)}$	$\frac{2E_Y}{3(1-\nu)K\varepsilon_0}$
Pini et al. (2009)	$\frac{3C_e}{K\varepsilon_0}$	$\frac{3C_sE_Y}{K\varepsilon_0}$

isotherms by assuming a constant value for the adsorbed phase density, i.e. 36.7 mol/L, 42.1 mol/L and 47.1 mol/L for CO_2, CH_4 and N_2, respectively. Values for the fitted parameters are reported in Table 1.

In principle, the parameters C_1 and C_2 in (6) can be estimated based on mechanical properties only, under the assumption of a specific simplified stress situation of the coal bed (Bustin et al. 2008). However, the history matching with field data or with laboratory experiments often requires the introduction of additional fitting parameters (Gilman and Beckie 2000; Shi and Durucan 2004; Pini et al. 2009). In Table 2 are reported the relationships for the constants C_1 and C_2 for these situations. With the known definition of the bulk modulus, i.e. $K = E_Y/[3(1-2\nu)]$, it can be seen that for all models, the input parameters are the two coal elastic properties, namely the Young's modulus E_Y and Poisson's ratio ν, respectively. In the model proposed by Gilman and Beckie (2000), E_f is some analogous of Young's modulus for a fracture, whereas in the model by Shi and Durucan (2004), C_f is defined as the fracture compressibility. Both parameters can be found by fitting them to experimental data. In an analogous way, in the model by Pini et al. (2009), which is also used in this study, experiments with a non-adsorbing (and non-swelling) gas, were used to obtain values for C_e, whereas experiments with an adsorbing gas were then used to estimate the values for the coefficient C_s (see next section for details).

Finally, the parameters needed for the Peng-Robinson EOS are given in Table 3.

3.2 Model evaluation

A situation representative for a coal bed lying at 500 m depth is described, whose properties are those of the Italian coal of the Sulcis Coal Province (Sardinia, Italy). The input parameters used for the model calculations are summarized in Tables 4 and 5. The coal bed permeability has been chosen to match typical values for coal seams, which usually lie between 1 and 10 mD (Gilman and Beckie 2000; White et al. 2005). For all the species a constant mass transfer coefficient of 10^{-5} s^{-1} has been chosen, corresponding to a sorption time constant $\tau = 1/k_{mi}$ of about 1.2 days, in agreement with values typically used in reservoir

Table 3 Thermodynamic properties of CO_2, CH_4 and N_2 for the Peng-Robinson EOS

Fluid	T_c [K]	P_c [MPa]	w [–]	k_{ij}		
				N_2	CH_4	CO_2
N_2	126.192	3.396	0.0372	0	0.031	−0.02
CH_4	190.56	4.599	0.0114	0.031	0	0.103
CO_2	304.13	7.377	0.224	−0.02	0.103	0

Table 4 Input parameters for the model

Property	Value
Temperature, T [°C]	45
Coal seam length, L [m]	100
Cross sectional area, A [m^2]	1
Initial pressure, P_0 [MPa]	1.5
Initial gas composition (% CH_4)	100
Initial unstressed permeability, k_0 [mD]	10
Initial unstressed cleat porosity, ε_0 [%]	8
Macropore porosity, ε_p [%]	2
Coal bulk density, ρ_s [kg/m^3]	1356.6
Mass transfer coeff., k_{mi} [s^{-1}]	10^{-5}
Sorption time, τ [days]	1.2
Injection pressure, P_{inj} [MPa]	4
Production pressure, P_{out} [MPa]	0.1

Table 5 Parameters for the permeability relationship (6)

Parameter	Shi and Durucan[a]	Bustin et al. (2008)	This study	
			Case A	Case B
ν [–]	0.35	0.3	0.26	0.26
E_Y [GPa]	2.62–2.90	3.00	1.12	1.12
ε_0 [–]	0.001–0.004	0.0023	0.08	0.08
C_f [GPa^{-1}]	116–290	–	–	–
C_e [–]	–	–	4.676	4.676
C_s [–]	–	–	0.622–2.377	2.5
C_1 [GPa^{-1}]	187.4–468.5	128.1–323.0	225.7	225.7
C_2 [–]	467.6–1293.9	197.0–496.9	33.6–128.4	134.4

[a]Refs. Shi and Durucan (2004, 2006); Shi et al. (2008)

simulators (Bromhal et al. 2005; Shi and Durucan 2005; Shi et al. 2008) and obtained from experiments performed under similar conditions (Pini et al. 2009). The injection pressure ($P_{\text{inj}} = 4$ MPa) is chosen to be slightly lower than the hydrostatic pressure corresponding to the coal seam depth (50 MPa) and the pressure at the production well is kept constant at a value of $P_{\text{out}} = 0.1$ MPa. Moreover, at the beginning of the injection, the reservoir pressure (100% CH_4) is lower than the hydrostatic pressure and takes a value of $P_0 = 1.5$ MPa, as might occur after the coal bed primary production.

Two cases have been investigated, which differ in the value of the parameter C_2 in (6), to highlight the effect of the permeability variation on the gas flow dynamics during the ECBM process. For "Case A", the values for the parameter $C_{\text{s},i}$ obtained for each component i from the experiments reported in Pini et al. (2009) have been used to calculate C_{s} defined as the weighted average among the three component, i.e. $C_{\text{s}} = \sum_{i=1}^{n_{\text{c}}} C_{\text{s},i} x_i$, with x_i being the fractional swelling (s_i/s). Values of $C_{\text{s},i}$ used for CO_2, CH_4 and N_2 are 0.623, 1.480 and 2.337, respectively. For "Case B", a four times larger value $C_{\text{s},i}$ has been set for CO_2 and has been used also for all other components. For this reason, we will refer to this situation as the strong swelling case. The value of these parameters are summarized in Table 5. For the sake of comparison, they are reported together with values given in other studies using a similar stress-strain relationship for the permeability. It is worth pointing out that the initial porosity values used in this work are much larger than those from other studies. This is mainly due to the fact that the reference condition (0) is different: in our study it refers to a unstressed state (no confinement, no fluid pressure), whereas in the other studies it refers to the initial reservoir condition, thus taking into account also the overburden stress.

As quantitative indicators to compare the outcomes of the different ECBM simulations, the following variables are defined (i =CH_4):

$$\text{GIP} = AL\left[\varepsilon^* c_i^0 + (1-\varepsilon^*) n_i^0\right] \tag{10a}$$

$$R_i = \frac{A \int_0^t u c_i \mid_{z=L} dt}{\text{GIP}} \tag{10b}$$

$$Pu_i = \frac{c_i \mid_{z=L}}{\sum_{j=1}^{n_{\text{c}}} c_j \mid_{z=L}} \tag{10c}$$

where GIP is the initial gas in place, R_i is the current value of the fraction of CH_4 recovered and Pu_i is its current purity. In the case of CO_2, the following variables are introduced (i =CO_2):

$$I_i = A \int_0^t u c_i \mid_{z=0} dt \tag{11a}$$

$$S_i = A \int_0^L \left[\varepsilon^* c_i + (1-\varepsilon^*) n_i\right] dz \tag{11b}$$

with I_i and S_i being the current amount injected and stored in the coal bed, respectively.

4 Results

4.1 Permeability behavior

By assuming that methane is completely displaced by the injected gas, the changes in permeability can be analytically estimated with (6) only. Figure 2 shows the obtained variations in permeability under different injection schemes (from pure CO_2 to pure N_2) for Cases A and B. In both cases the confining pressure (P_{c}) has been kept constant at a value of 10 MPa. In the figure, the predicted injection curves are compared to the primary recovery scenario (pure CH_4, dashed line), for which the coal bed situation before starting gas injection is marked with a circle. The vertical dotted line at 4 MPa represents a theoretical abandonment scenario, where, at the end of the ECBM operation, the coal seam has

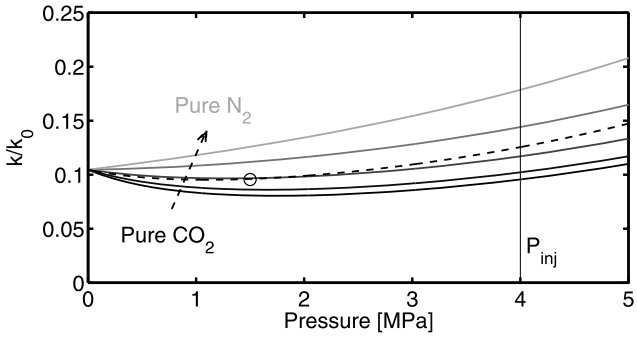

(a) Case A - weak swelling

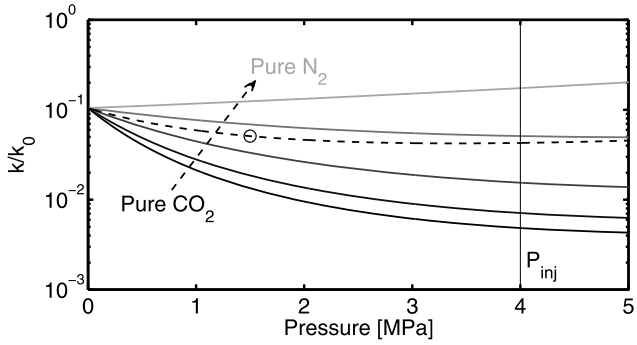

(b) Case B - strong swelling

Fig. 2 Permeability ratio k/k_0 as a function of pressure P under different injection scenarios (*solid lines*, Pure CO_2, 80:20/CO_2:N_2, 50:50/CO_2:N_2, 20:80/CO_2:N_2, pure N_2) for Case A (weak swelling) (**a**) and Case B (strong swelling) (**b**). The *dashed line* corresponds to the primary recovery scenario (pure CH_4) and the *empty circle* to the initial condition in the reservoir

been completely filled with the injected gas at a pressure corresponding to the injection pressure. Qualitatively there is no difference between Case A and B: pure CO_2 injection leads to the strongest reduction in permeability, whereas addition of N_2 to the mixture allows counteracting this effect. At constant pressure, the difference in the permeability behavior among the different injection scenarios depends on the extent of swelling of the coal, which is fluid dependent. Because of the weak sorption and swelling of N_2 compared to CH_4 and CO_2 (see Fig. 1), the injection of CO_2/N_2 mixtures induces less permeability reduction compared to pure CO_2. For gas mixtures rich in N_2, permeability can be even larger when compared to the initial situation. Moreover, due to the larger swelling constant (C_2), in Case B the changes in permeability are more pronounced compared to Case A. In particular, in Case B permeability can either be enhanced or reduced of about one order of magnitude, depending on whether pure N_2 or CO_2 is injected. Finally, in agreement with observation reported in previous studies, for Case A a characteristic minimum in permeability can be clearly seen that is positioned at the so-called rebound pressure (Palmer and Mansoori 1998; Shi et al. 2008; Pini et al. 2009). For Case B the rebound doesn't appear in the pressure range investigated due to the imposed stronger swelling.

In the following, ECBM simulations results are presented for which the permeability behavior just described has been used as an input to the model. First, some important characteristic features of gas displacement and storage during ECBM recovery are shown for the case of pure CO_2 injection (Sect. 4.2). Then, a number of ECBM schemes involving the injection of CO_2/N_2 gas mixtures with different composition are investigated and compared in terms of performance of the ECBM/CO_2 recovery operation (Sect. 4.3). For the sake of better clarity, Case A has been assumed for the simulations presented in Sect. 4.2 and 4.3. Finally, the effect of swelling is investigated and a comparison between Cases A and B is shown in Sect. 4.4.

4.2 ECBM with pure CO_2

The two main peculiarities of the ECBM recovery process are that the adsorption/desorption mechanism taking place controls the displacement dynamics and that gas sorption is responsible for gas storage in coal seams. Figure 3a shows a snapshot of the composition profiles of CO_2 (solid line) and CH_4 (dashed line) in the coal bed at two different times (16 and 83 days), whereas Fig. 3b shows the corresponding pressure profiles. It can be seen that injection of pure CO_2 displaces the CH_4 through a relatively sharp front, due to the higher adsorptivity of the former compared to the latter. Therefore as the preferentially adsorbing CO_2 propagates through the coal bed, no CH_4 is left behind. Moreover,

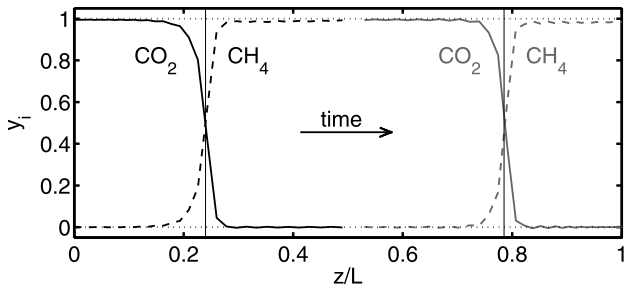

(a) Composition profiles

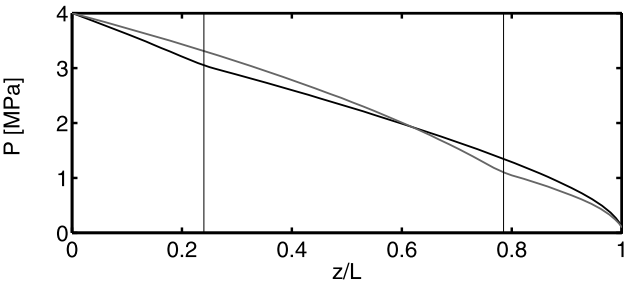

(b) Pressure profiles

Fig. 3 ECBM with pure CO_2 injection (Case A): composition profiles (**a**) and pressure profiles (**b**) along the coal seam axis calculated at two different times during CH_4 displacement by pure CO_2 injection

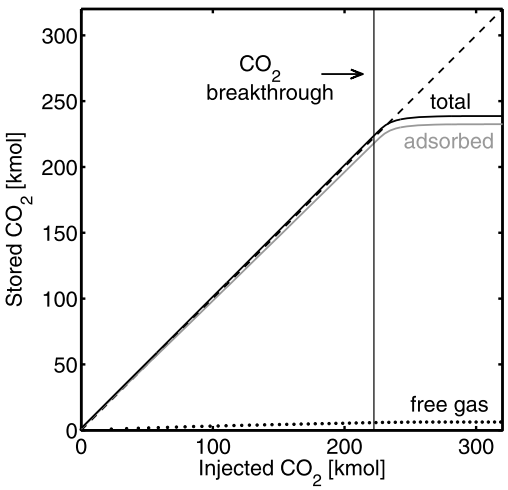

Fig. 4 Amount of CO_2 stored as a function of the amount of CO_2 injected in the coal bed during CH_4 displacement by pure CO_2 injection (Case A). The amount of CO_2 stored in the reservoir is further classified as free gas (*dotted line*) and adsorbed gas (*gray line*)

the shape of the composition profiles remains constant in time, whereas the one of the pressure profiles varies slightly and shows a characteristic bending at the position of the displacement front; the reason for this can be attributed to gas volume changes associated with the adsorption/desorption process.

Figure 4 shows the amount of CO_2 stored in the coal bed (S_{CO2}), as a function of the amount of CO_2 injected (I_{CO2}).

It can be seen that as long as breakthrough doesn't occur the amount of gas stored in the coal bed equals the amount of gas injected, as it should be just from the point of view of mass conservation (dashed line). However, at breakthrough the curve bends and reaches a constant value as adsorption has also reached equilibrium and the coal is saturated. The time (or amount of gas) needed from breakthrough to reach this point depends on the value of the mass transfer coefficient in (3) and takes a value of zero when local equilibrium between fluid and adsorbed phase is assumed (Zhu et al. 2003). Finally, it can be seen that indeed the amount of CO_2 adsorbed (gray line) accounts for the majority of the storage (black line), whereas the contribution of gas storage in the fractures and in the macropores (dotted line) is minor.

4.3 Effects of injected gas composition

Figure 5 shows the composition profiles of CO_2, CH_4 and N_2 along the coal bed axis after 42 days for three different injection scenarios: pure CO_2 (a), 50:50/CO_2:N_2 (b) and pure N_2 (c). It can be seen that, differently from the sharp front described in the previous section, when pure N_2 is injected the displacement front is much smoother, with the N_2 moving faster than CH_4 and overtaking it. Again, this can be attributed to the adsorption behavior of the gases involved, as in this case the injected component (N_2) adsorbs less than the displaced component (CH_4). Injection of a CO_2/N_2 mixture results in the appearance of both the above mentioned effects, as shown in the central figure. In particular, at the CO_2/CH_4 front the N_2 is enriched in the fluid phase, the latter being the least adsorbing component.

Figure 6 shows the flow rates of CO_2, CH_4 and N_2 at the production well corresponding to the three different scenarios just described. It can be seen that when pure CO_2 is injected, the CH_4 recovery is completed as CO_2 breakthrough takes place, because of the characteristic displacement behavior described above. On the contrary, gas mixtures containing N_2 show an early breakthrough of N_2. In the case of 50:50/CO_2:N_2 injection, this results in a produced stream of CH_4 polluted with N_2, until CO_2 breakthrough occurs. It is worth noting that in all cases, the initial rapid decrease in the rate of produced CH_4 is due to the opening of the production well that leads to a decrease of the pressure from the initial value (1.5 MPa) to the imposed boundary condition (0.1 MPa). From a practical point of view, the end of the operation in the case of pure CO_2 injection is determined by the CO_2 breakthrough, whereas in the case of pure N_2 injection it will depend on the purity of the produced CH_4.

These concepts can be better visualized with the help of Figs. 7a and 7b, where the produced gas quality (in terms of CH_4 purity) (a) and the amount of CH_4 recovered (b) are shown as a function of the cumulative amount

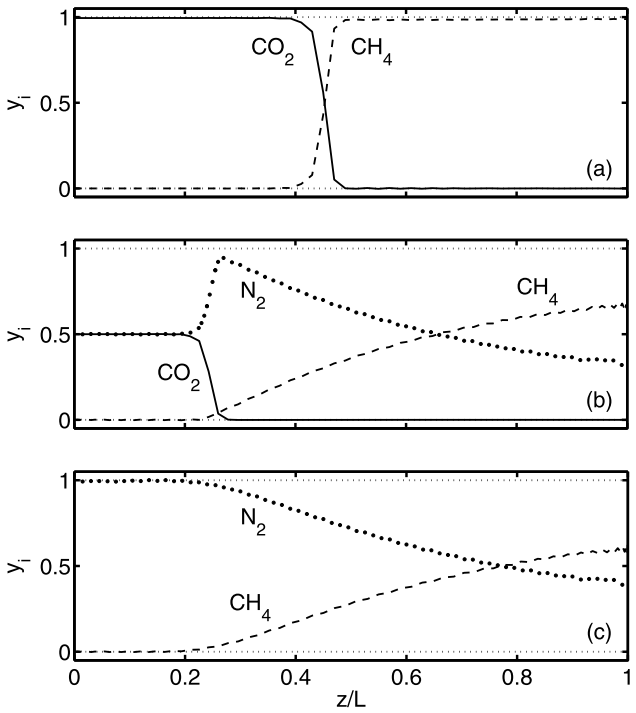

Fig. 5 Composition profiles of CO_2, CH_4 and N_2 along the coal bed axis for three different injection scenarios: pure CO_2 (**a**), 50:50/CO_2:N_2 (**b**) and pure N_2 (**c**)

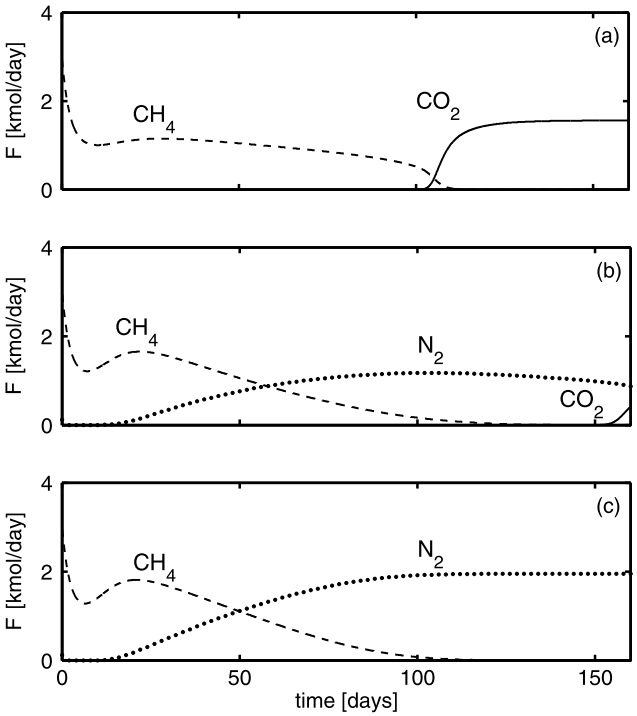

Fig. 6 Flow rates of CO_2, CH_4 and N_2 at the production well as a function of time for three different injection scenarios: pure CO_2 (**a**), 50:50/CO_2:N_2 (**b**) and pure N_2

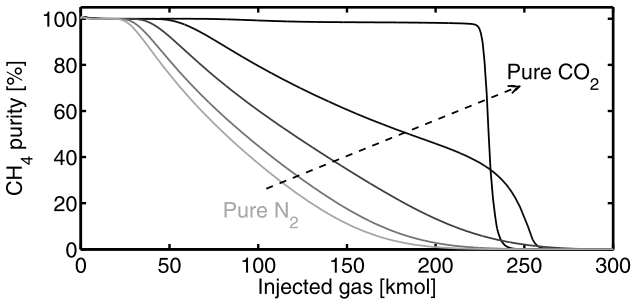

(a) Methane purity

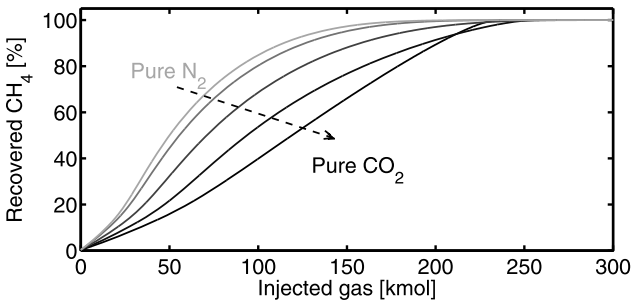

(b) Methane recovery

Fig. 7 Enhanced coal bed methane recovery: CH_4 purity (**a**) and CH_4 recovery (**b**) as a function of the amount of injected gas for different ECBM schemes with different injection compositions (Pure CO_2, 80:20/CO_2:N_2, 50:50/CO_2:N_2, 20:80/CO_2:N_2 and pure N_2)

of gas injected for different ECBM injection scenarios. Note that since for these simulations a constant injection pressure ($P_{inj} = 4$ MPa) boundary condition was imposed, the use of the cumulative gas injection as the x-coordinate instead of time is more appropriate. It can be clearly seen that addition of N_2 into the injected gas results in an increased pollution of the methane produced, due to overlapping between the N_2 injection front and the CH_4 desorption front described previously. In the case of pure CO_2, the produced gas is pure CH_4 until completion of the recovery process. Moreover, with respect to the amount of CH_4 recovered, injection of N_2-rich gas mixtures allows for a faster initial CH_4 recovery compared to the case where pure CO_2 is injected. However, the total CH_4 recovery is achieved earlier with increasing CO_2 content in the feed, as shown by the crossover appearing at large CH_4 recovery values. This behavior can be explained by the very effective CH_4 displacement achieved with CO_2 (due to its larger adsorptivity compared to both CH_4 and N_2). Results that show a similar crossover have been observed by assuming constant porosity and permeability and by applying the method of characteristics to obtain analytical solutions of gas transport during ECBM recovery (Zhu et al. 2003; Seto et al. 2009). Here, the slower initial recovery observed when CO_2-rich mixtures are injected was attributed to a reduction in the local flow velocity caused by the removal of CO_2 from the fluid (mobile) phase.

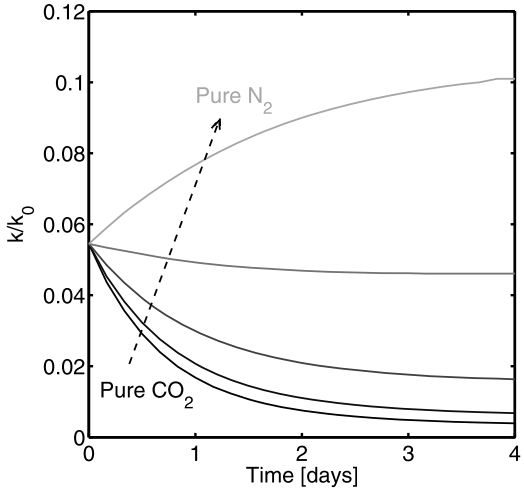

Fig. 8 Permeability ratio k/k_0 at the injection well as a function of time for Case B (strong swelling) for different ECBM schemes with different injection compositions (Pure CO_2, 80:20/CO_2:N_2, 50:50/CO_2:N_2, 20:80/CO_2:N_2 and pure N_2)

4.4 Effects of swelling and permeability

Field tests have shown that CO_2 injection yields to injectivity problems caused by the reduction in permeability (Gunter et al. 2004; Reeves 2004; van Bergen et al. 2006). Moreover, it is expected that the main loss in permeability is confined around the injection well, where the CO_2 concentration is the highest. Figure 8 shows the permeability ratio k/k_0 at the injection well ($z = 0$) as a function of time for Case B during the first 4 days of injection. For pure CO_2, the initial permeability takes a value of about 4.4 mD and after 4 days permeability has dropped down to 0.4 mD, corresponding to a reduction of about one order of magnitude. For pure N_2, the situation is reversed, with almost a doubling of the initial permeability value. The situations where a gas mixture is injected lie between these two limiting cases.

This reduction in permeability can have serious effects on the ECBM operation itself. Figure 9a and 9b show the amount of CO_2 injected in the coal bed as a function of time for the different ECBM schemes for the situations where swelling is weak (Case A) and strong (Case B), respectively. For Case A, it can be seen that the obtained curves are fanning out; this result is not surprising as the use of a CO_2-rich mixture clearly leads to an increased amount of CO_2 injected. However, for Case B the difference between the four injection scenarios is much smaller compared to Case A. In other words, the increase in the CO_2 feed concentration is not reflected into a corresponding larger amount of CO_2 injected, and this is particularly evident for the pure CO_2 case when compared to the 80:20/CO_2:N_2 case. An interesting scenario arises from these results: even if the goal is to maximize the storage of CO_2, it could be more effective to inject a mixture of CO_2/N_2 instead of pure CO_2.

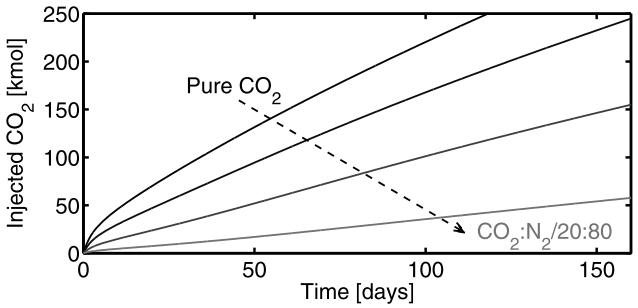

(a) Case A - weak swelling

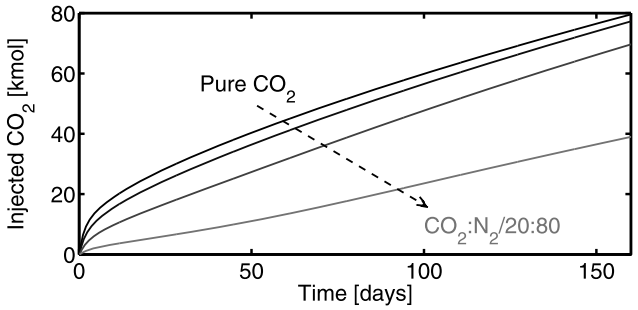

(b) Case B - strong swelling

Fig. 9 Amount of CO_2 injected as a function of time for Case A (weak swelling) (**a**) and Case B (strong swelling) (**b**) for different ECBM schemes with different injection compositions (Pure CO_2, 80:20/CO_2:N_2, 50:50/CO_2:N_2 and 20:80/CO_2:N_2)

5 Discussion

Gas is retained in coal seam primarily by the mechanism of gas sorption. The results presented in Sect. 4.2 show that indeed gas sorption accounts for more than 95% of the total amount of CO_2 stored in the coal bed. Moreover, since the density of gas in the adsorbed state is higher (liquid-like) compared to its corresponding equilibrium density in the gas phase, adsorption represents a more efficient way of storage than gas compression. It is usually assumed that at similar depth and pressure, coal beds may contain 2–4 times the amount of gas contained in a conventional gas reservoir (McElhiney et al. 1993). From the point of view of coal bed gas production, this gives rise to typical production curves that are characterized by low production pressures in order to allow for significant gas desorption to take place (Schraufnagel 1993). A similar concept can be applied to CO_2 storage in coal seams: a significant reservoir pressure loss has to occur before gas desorption from the coal matrix can actually start; this is particularly true for a Langmuir-like isotherm, which has been shown to provide an effective description of gas sorption in coal (Pini et al. 2010). Moreover, the gas release from the coal matrix is controlled by the desorption rate, which for some deep coal beds is determined by sorption times as high as 70 days (McElhiney et al. 1993). In this context, gas sorption represents therefore an obstacle to gas leakage from these geological formations. This conclusion is supported by observing that coal bed methane can be produced today, even if it has been generated during the seam formation, a process which might have taken millions of years.

The recovery of the CH_4 that is naturally present in the coal bed is achieved through an in situ adsorption/desorption process. In Sect. 4.3 different injection scenarios have been investigated, including the injection of pure CO_2, pure N_2 or mixtures into a coal bed previously saturated with methane, the latter being attractive as it would allow injecting flue gas directly without the expensive CO_2 capture step. With respect to the recovery of the original gas in place, interesting results have been obtained in terms of purity and production rate, which could be understood by looking at the specific adsorption behavior of each component on the coal. When a component is chosen that adsorbs more than methane, such as CO_2, the initial recovery is slower, but the displacement is more effective, thus allowing for a faster total recovery. On the contrary, the less adsorbing N_2 allows for a fast initial CH_4 recovery, despite its earlier breakthrough that pollutes the produced CH_4. From a practical point of view therefore, if one is interested in the recovered methane as a fuel or a technical gas, there is a clear trade-off between the incremental methane recovery that can be achieved and the quality of the produced gas. However, if the goal is that of storing CO_2 that has been captured, then the amount of CO_2 that can be injected and stored in the reservoir is of primary importance.

The volume change of the coal associated with gas sorption can change substantially the picture just described. It was shown in Sect. 4.4 that the strong permeability reduction caused by the swelling of the coal when exposed to CO_2 has serious implications on the performance of an ECBM operation. In particular, the simulation results for Case B show that the use of a mixture with composition 80:20/CO_2:N_2 allows injecting (and therefore storing) a similar amount of CO_2 as when pure CO_2 is used. The swelling and the resulting closing of the fractures will initially affect the region close to the injection well, where the CO_2 is the highest, therefore impeding the exploitation of the whole coal bed volume. In agreement with observations from previous simulation studies (Durucan and Shi 2009), the results obtained in this work disclose new routes towards several attractive options aimed at tackling the injectivity problem just described and that need to be further investigated. These include the use of flue gas as a way of keeping the permeability sufficiently high, as well as the development of design criteria in terms of configuration of injection and production wells (multi-well pattern), as a way of maximizing CO_2 storage and CH_4 recovery.

6 Concluding remarks

In this study, the gas flow dynamics during ECBM recovery operations have been studied with the help of a one-dimensional mathematical model, consisting of mass balances describing gas flow and sorption, and a geomechanical relationship for the description of porosity and permeability changes during injection. Simulation results show that gas injection can indeed enhance methane recovery. Moreover, when N_2 is injected, an initially much more rapid response in terms of methane recovery is observed, whereas the strong adsorbing CO_2 yields for a more effective displacement and therefore for a faster total recovery of methane. Coal swelling plays a major role in controlling the ECBM recovery process: the closing of the fractures associated with it strongly reduces coal's permeability. In this context, flue gas injection might represent an attractive option, as it would keep permeability sufficiently high, with the constraint that the N_2 injection front and the CH_4 desorption front overlap so as the injected gas pollutes methane much more than in the case of pure CO_2 injection. The results of the present study suggest therefore that there is room for optimizing the ECBM process depending on whether the objective of the project is to maximize the CO_2 storage or the methane recovery.

The 1-D description presented above provides a very useful understanding of the key mechanisms that affect the storage and recovery process. However, the 1-D model presented in this study has to be extended to a 3-D domain, if the goal is to history-match field tests data. Moreover, efforts in this direction should account for the presence of water in the coal bed (multiphase flow), for the complexity of the coal's pore structure that impacts also mass transfer mechanisms, and finally for the heterogeneity in the chemical and mechanical properties of the coal that is present at the reservoir scale. When considering innovative injection policies, e.g. direct flue gas injection instead of injection of captured CO_2, a careful economic evaluation that includes the compression costs has to be carried out. We believe that in this context the availability of the characterization tools and protocols exploited here and of the 1-D model presented in this work will play an important role.

References

Bae, J.S., Bhatia, S.K.: High-pressure adsorption of methane and carbon dioxide on coal. Energy Fuels **20**(6), 2599–2607 (2006)

Bromhal, G.S., Neal Sams, W., Jikich, S., Ertekin, T., Smith, D.H.: Simulation of CO_2sequestration in coal beds: The effects of sorption isotherms. Chem. Geol. **217**(3–4), 201–211 (2005)

Bustin, R.M., Cui, X.J., Chikatamarla, L.: Impacts of volumetric strain on CO_2 sequestration in coals and enhanced CH_4recovery. Am. Assoc. Pet. Geol. Bull. **92**(1), 15–29 (2008)

Cui, X.J., Bustin, R.M., Chikatamarla, L.: Adsorption-induced coal swelling and stress: Implications for methane production and acid gas sequestration into coal seams. J. Geophys. Res. **112**, B10202 (2007)

Day, S., Duffy, G., Sakurovs, R., Weir, S.: Effect of coal properties on CO_2sorption capacity under supercritical conditions. Int. J. Greenh. Gas Control **2**(3), 342–352 (2008a)

Day, S., Fry, R., Sakurovs, R.: Swelling of Australian coals in supercritical CO_2. Int. J. Coal Geol. **74**(1), 41–52 (2008b)

Durucan, S., Shi, J.Q.: Improving the CO_2 well injectivity and enhanced coalbed methane production performance in coal seams. Int. J. Coal Geol. **77**(1–2), 214–221 (2009)

Gentzis, T.: Subsurface sequestration of carbon dioxide—an overview from an Alberta (Canada) perspective. Int. J. Coal Geol. **43**(1–4), 287–305 (2000)

Gilman, A., Beckie, R.: Flow of coal-bed methane to a gallery. Transp. Porous Media **41**(1), 1–16 (2000)

Gray, I.: Reservoir engineering in coal seams. Part 1. The physical process of gas storage and movement in coal seams. SPE Reservoir Engineering SPE Paper **12514**, 28–34 (1987)

Gunter, W.D., Mavor, M.J., Robinson, J.R.: CO_2storage and enhanced methane production: field testing at the Fenn-Big Valley, Alberta, Canada, with application. In: Rubin, E., Keith, D., Gilboy, C., Wilson, M., Morris, T., Gale, J., Thambimuthu, K. (eds.) Proceedings of the 7th International Conference on Greenhouse Gas Control Technologies, Vancouver, Canada, September 5–9, vol. 1, pp. 413–421 (2004)

IEA: World Energy Outlook—Executive Summary. Paris-Cedex, France (2009)

IPCC: IPCC Special Report on Carbon Dioxide Capture and Storage. Prepared by Working Group III of the Intergovernmental Panel on Climate Change [Metz, B., O. Davidson, H.C. de Coninck, M. Loos, and L.A. Meyer (eds.)]. Cambridge University Press, Cambridge (2005)

Jessen, K., Tang, G.Q., Kovscek, A.: Laboratory and simulation investigation of enhanced coalbed methane recovery by gas injection. Transp. Porous Media **73**(2), 141–159 (2008)

Levine, J.: Model study of the influence of matrix shrinkage on absolute permeability of coal bed reservoirs. In: Gayer, R., Harris, I. (eds.) Coalbed Methane and Coal Geology, vol. 109, pp. 197–212. Geological Society, London (1996), Special Publication

Mazumder, S., Wolf, K.H.: Differential swelling and permeability change of coal in response to CO_2 injection for ECBM. Int. J. Coal Geol. **74**(2), 123–138 (2008)

Mazzotti, M., Pini, R., Storti, G.: Enhanced coal bed methane recovery. J. Supercrit. Fluids **47**(3), 619–617 (2009)

McElhiney, J.E., Paul, G.W., Young, G.B.C., McCartney, J.A.: Reservoir engineering aspects of coalbed methane. In: Law, B., Rice, D. (eds.) Hydrocarbons from Coal. AAPG Studies in Geology, vol. 38, pp. 361–372. American Association of Petroleum Geologists, Tulsa (1993)

Morbidelli, M., Servida, A., Storti, G.: Application of the orthogonal collocation method to some chemical engineering problems. Ing. Chi. Ital. **19**(5–6), 46–60 (1983)

Ottiger, S., Pini, R., Storti, G., Mazzotti, M., Bencini, R., Quattrocchi, F., Sardu, G., Deriu, G.: Adsorption of pure carbon dioxide and methane on dry coal from the Sulcis Coal Province (SW Sardinia, Italy). Environ. Prog. **25**(4), 355–364 (2006)

Ottiger, S., Pini, R., Storti, G., Mazzotti, M.: Competitive adsorption equilibria of CO_2 and CH_4 on a dry coal. Adsorption **14**(4–5), 539–556 (2008)

Palmer, I., Mansoori, J.: How permeability depends on stress and pore pressure in coalbeds: A new model. SPE Reserv. Evalu. Eng. **1**(6), 539–544 (1998)

Peng, D.Y., Robinson, D.B.: A new two-constant equation of state. Ind. Eng. Chem. Fundam. **15**(1), 59–64 (1976)

Pini, R., Ottiger, S., Burlini, L., Storti, G., Mazzotti, M.: Role of adsorption and swelling on the dynamics of gas injection in coal. J. Geophys. Res. **114**, B04203 (2009)

Pini, R., Ottiger, S., Burlini, L., Storti, G., Mazzotti, M.: Sorption of carbon dioxide methane and nitrogen in dry coals at high pressure and moderate temperature. Int. J. Greenh. Gas Control **4**(1), 90–101 (2010)

Reeves, S.R.: The Coal-Seq project: Key results from field, laboratory, and modeling studies. In: Rubin, E., Keith, D., Gilboy, C., Wilson, M., Morris, T., Gale, J., Thambimuthu, K. (eds.) Proceedings of the 7th International Conference on Greenhouse Gas Control Technologies, Vancouver, Canada, September 5–9, vol. II, pp. 1399–1403 (2004)

Reid, R.C., Prausnitz, J.M., Poling, B.E.: The Properties of Gases and Liquids, 4th edn. McGraw-Hill, New York (1987)

Rice, D.D.: Composition and origins of coalbed gas. In: Law, B., Rice, D. (eds.) Hydrocarbons from Coal. AAPG Studies in Geology, vol. 38, pp. 159–184. American Association of Petroleum Geologists, Tulsa (1993)

Sams, W.N., Bromhal, G., Jikich, S., Ertekin, T., Smith, D.H.: Field-project designs for carbon dioxide sequestration and enhanced coalbed methane production. Energy Fuels **19**(6), 2287–2297 (2005)

Schraufnagel, R.A.: Coalbed methane production. In: Law, B., Rice, D. (eds.) Hydrocarbons from Coal. AAPG Studies in Geology, vol. 38, pp. 341–359. American Association of Petroleum Geologists, Tulsa (1993)

Seto, C.J., Jessen, K., Orr, F.M., Jr.: A multicomponent two-phase-flow model for CO_2 storage and enhanced coalbed-methane recovery. Soc. Pet. Eng. J. **14**(1), 30–40 (2009)

Shi, J.Q., Durucan, S.: A bidisperse pore diffusion model for methane displacement desorption in coal by CO_2 injection. Fuel **82**(10), 1219–1229 (2003)

Shi, J.Q., Durucan, S.: Drawdown induced changes in permeability of coalbeds: A new interpretation of the reservoir response to primary recovery. Transp. Porous Media **56**(1), 1–16 (2004)

Shi, J.Q., Durucan, S.: Gas storage and flow in coalbed reservoirs: Implementation of a bidisperse pore model for gas diffusion in a coal matrix. SPE Reserv. Evalu. Eng. **8**(2), 169–175 (2005)

Shi, J.Q., Durucan, S.: The assessment of horizontal well option for CO_2 storage and ECBM recovery in unmineable thin seams: Pure CO_2 vs. CO_2 enriched flue gas. In: Proceedings of the 8th International Conference on Greenhouse Gas Control Technologies, Trondheim, Norway, June 19–22 (2006)

Shi, J.Q., Durucan, S., Fujioka, M.: A reservoir simulation study of CO_2 injection and N_2 flooding at the Ishikari coalfield CO_2 storage pilot project. Jpn. Int. J. Greenh. Gas Control **2**(1), 47–57 (2008)

St. George, J.D., Barakat, M.A.: The change in effective stress associated with shrinkage from gas desorption in coal. Int. J. Coal Geol. **45**(2–3), 105–113 (2001)

Totsis, T.T., Patel, H., Najafi, B.F., Racherla, D., Knackstedt, M.A., Sahimi, M.: Overview of laboratory and modeling studies of carbon dioxide sequestration in coal beds. Ind. Eng. Chem. Res. **43**, 2887–2901 (2004)

van Bergen, F., Pagnier, H., Krzystolik, P.: Field experiment of CO_2-ECBM in the Upper Silesian Basin of Poland. In: Proceedings of the 8th International Conference on Greenhouse Gas Control Technologies, Trondheim, Norway, June 19–22 (2006)

van Bergen, F., Krzystolik, P., van Wageningen, N., Pagnier, H., Jura, B., Skiba, J., Winthaegen, P., Kobiela, Z.: Production of gas from coal seams in the Upper Silesian Coal Basin in Poland in the post-injection period of an ECBM pilot site. Int. J. Coal Geol. **77**(1–2), 175–187 (2009)

Villadsen, J., Michelsen, M.L.: Solution of Differential Equation Models by Polynomial Approximation. Prentice-Hall International Series in the Physical and Chemical Engineering Science. Englewood Cliffs, Prentice-Hall (1978)

Wang, F.Y., Zhu, Z.H., Massarotto, P., Rudolph, V.: Mass transfer in coal seams for CO_2 sequestration. AlChE J. **53**(4), 1028–1049 (2007)

White, C.M., Smith, D.H., Jones, K.L., Goodman, A.L., Jikich, S.A., LaCount, R.B., DuBose, S.B., Ozdemir, E., Morsi, B.I., Schroeder, K.T.: Sequestration of carbon dioxide in coal with enhanced coalbed methane recovery—a review. Energy Fuels **19**(3), 659–724 (2005)

Zhu, J., Jessen, K., Kovscek, A.R., Orr, F.M., Jr.: Analytical theory of coalbed methane recovery by gas injection. Soc. Pet. Eng. J. **8**(4), 371–379 (2003)